The Astrophysical Journal Letters, 725:L181–L185, 2010 December 20 doi:10.1088/2041-8205/725/2/L181

IDENTIFICATION OF KCN IN IRC+10216: EVIDENCE FOR SELECTIVE CYANIDE CHEMISTRY

R. L. Pulliam[1], C. Savage[2], M. Agúndez[3], J. Cernicharo[4], M. Guélin[5], and L. M. Ziurys[1,6]
[1] Department of Astronomy, Department of Chemistry and Steward Observatory, University of Arizona, 933 North Cherry Avenue, Tucson, AZ 85721, USA
[2] Applied Electromagnetics (IAT-2), Los Alamos National Laboratory, Los Alamos, NM 87545, USA
[3] LUTH, Observatoire de Paris-Meudon, 5 Place Jules Janssen, 92190 Meudon, France
[4] Departamento de Astrofísica, Centro de Astrobiología, CSIC-INTA, Ctra. De Torrejón a Ajalvir km 4, 28850 Madrid, Spain
[5] Institut de Radioastronomie Millimétrique, 300 rue de la Piscine, 38406 Saint Martin d'Hères, France
[6] Arizona Radio Observatory, University of Arizona, 933 North Cherry Avenue, Tucson, AZ 85721, USA
Received 2010 October 13; accepted 2010 November 10; published 2010 December 2

ABSTRACT

A new interstellar molecule, KCN, has been identified toward the circumstellar envelope of the carbon-rich asymptotic giant branch star, IRC+10216—the fifth metal cyanide species to be detected in space. Fourteen rotational transitions of this T-shaped, asymmetric top were searched for in the frequency range of 83–250 GHz using the Arizona Radio Observatory (ARO) 12 m Kitt Peak antenna, the IRAM 30 m telescope, and the ARO Submillimeter Telescope. Distinct lines were measured for 10 of these transitions, including the $K_a = 1$ and 2 asymmetry components of the $J = 11 \rightarrow 10$ and $J = 10 \rightarrow 9$ transitions, i.e., the *K*-ladder structure distinct to an asymmetric top. These data are some of the most sensitive astronomical spectra at $\lambda \sim 1$ and 3 mm obtained to date, with 3σ noise levels ∼0.3 mK, made possible by new ALMA technology. The line profiles from the ARO and IRAM telescopes are consistent with a shell-like distribution for KCN with $r_{\rm outer} \sim 15''$, but with an inner shell radius that extends into warmer gas. The column density for KCN in IRC+10216 was found to be $N_{\rm tot} \approx 1.0 \times 10^{12}$ cm^{-2} with a rotational temperature of $T_{\rm rot} \sim 53$ K. The fractional abundance was calculated to be $f({\rm KCN/H_2}) \sim 6 \times 10^{-10}$, comparable to that of KCl. The presence of KCN in IRC+10216, along with MgNC, MgCN, NaCN, and AlNC, suggests that cyanide/isocyanide species are the most common metal-containing molecules in carbon-rich circumstellar gas.

Key words: astrochemistry – circumstellar matter – line: identification – stars: AGB and post-AGB – stars: individual (IRC +10216)

Online-only material: color figures

1. INTRODUCTION

It was once thought that the chemistry of circumstellar envelopes of evolved stars such as IRC+10216 consisted of only carbon, oxygen, nitrogen, and silicon-based compounds. Exotic gas-phase species containing refractory-type elements such as Na, Fe, Al, Mg, and K were thought to only exist in the hot photospheres of stars and to quickly condense into dust grains as photospheric material is lost to the cooler circumstellar shell (Tsuji 1973; Sofia et al. 1994). However, observations over the last 20 years have proven that this proposed scenario is overly simplified. Since 1987, a series of metal-containing molecules have been identified in circumstellar gas, beginning with the detection of the metal halide species NaCl, AlCl, KCl, and AlF in the carbon-rich shell of IRC+10216 (Cernicharo & Guélin 1987). These startling discoveries were subsequently followed by the identification of a series of cyanide/isocyanide compounds in IRC+10216: MgNC (Kawaguchi et al. 1993), NaCN (Turner et al. 1994), MgCN (Ziurys et al. 1995), and AlNC (Ziurys et al. 2002). Several of these molecules were then found in the circumstellar material of CRL2688 and CRL 618, both protoplanetary nebulae (Highberger et al. 2001, 2003; Highberger & Ziurys 2003). More recent work has revealed the presence of NaCl, AlO, and AlOH in oxygen-rich circumstellar shells such as VY Canis Majoris (e.g., Tenenbaum & Ziurys 2009, 2010; Tenenbaum et al. 2010a, 2010b).

Although the existence of metal halides and oxides had been predicted by early models of photospheric and inner shell chemistry (Tsuji 1973), the observation of cyanide species was not expected. Moreover, several of the metal cyanides appear to be primarily located in the outer circumstellar shell, as measurements of MgCN, MgNC, and AlNC have indicated (e.g., Guélin et al. 1993; Ziurys 2006). This region of the circumstellar envelope is ∼100–1000 stellar radii distant from the dust formation zone, where the gas has become quite cold ($T_K \sim 25$ K). Survival of these refractory molecules is surprising. In contrast, the metal halides, oxides, and even hydroxides are inner shell species, likely produced by LTE chemistry near the photosphere (Ziurys 2006; Tenenbaum & Ziurys 2009, 2010). However, the cyanide NaCN is also thought to be confined to the inner shell, at least in IRC+10216 (Turner et al. 1994; Ziurys 2006), and gas-phase atomic metals are observed in the cold outer regions of the same source (Mauron & Huggins 2010). It is clear that the chemistry of metals in the circumstellar envelopes of stars is not yet understood.

One molecule postulated to exist in IRC+10216 is the metal cyanide KCN, given the presence of KCl in this source. The millimeter spectrum of KCN, a T-shaped asymmetric top, has been known since 1980 (Törring et al. 1980). Since 2001, there have been various observations (e.g., Savage et al. 2003; Cernicharo et al. 2004; Patel et al. 2009) suggesting that KCN is present in IRC+10216, but a definitive detection has never been published. In order to clarify this situation, we have conducted a renewed search for this molecule, taking advantage of the improved sensitivity offered by ALMA-type mixers. We have observed 14 transitions of KCN, primarily in the $K_a = 0$ series. While emission was detected at all frequencies observed, 10 transitions were found to be relatively clear of confusion. Several of these transitions were observed at both the IRAM 30 m and Arizona Radio Observatory (ARO) 12 m telescopes. These spectra unambiguously indicate the presence of KCN in IRC+10216. In this Letter, we present our observations

Table 1
Observed Line Parameters for KCN in IRC+10216

Transition	Frequency (MHz)	θ_b ($''$)	η^a	$T_R{}^b$ (mK)	V_{LSR} (km s^{-1})	$\Delta V_{1/2}$ (km s^{-1})
$9_{0,9} \rightarrow 8_{0,8}$	84991.50	74	0.90	$\sim$0.8[c]	~ -26	...
$9_{1,9} \rightarrow 8_{1,8}$	83377.54	29	0.82	$\sim$2.3[c,d]	~ -24	...
$10_{0,10} \rightarrow 9_{0,9}$	94360.11	67	0.89	1.2 ± 0.3	-26.0 ± 3.2	25.4 ± 3.2
		26	0.81	3.3 ± 1.2[d]	-24.6 ± 3.0	32.0 ± 2.5
$10_{1,9} \rightarrow 9_{1,8}$	96649.20	26	0.80	6 ± 1.5[d,f]	~ -26	...
$10_{1,10} \rightarrow 9_{1,9}$	92621.12	27	0.81	3.9 ± 1.4[d]	-25.8 ± 3.0	25.2 ± 2.5
$11_{1,11} \rightarrow 10_{1,10}$	101858.59	62	0.88	1.0 ± 0.3	-23.0 ± 5.9	23.6 ± 5.9
$11_{0,11} \rightarrow 10_{0,10}$	103705.90	61	0.87	0.8 ± 0.5	-25.7 ± 2.9	28.9 ± 5.8
$11_{1,10} \rightarrow 10_{1,9}$	106285.47	59	0.86	0.9 ± 0.3	-26.8 ± 5.6	22.6 ± 5.6
		23	0.74	4.1 ± 1.5[d]	-26.0 ± 2.3	28.2 ± 2.3
$11_{2,10} \rightarrow 10_{2,9}$	104092.63	24	0.79	2.0 ± 0.7[d]	-21.9 ± 4.0	31.8 ± 2.5
$14_{0,14} \rightarrow 13_{0,13}$	131590.30	48	0.80	2.0 ± 0.5	-26.0 ± 4.6	31.9 ± 4.6
		19	0.72	6.5 ± 1.5[d]	-26.0 ± 2.3	27.4 ± 2.3
$15_{0,15} \rightarrow 14_{0,14}$	140830.81	45	0.80	...[e]	...	...
$16_{0,16} \rightarrow 15_{0,15}$	150043.30	42	0.75	3.0 ± 1.2	-26.1 ± 4.0	20.0 ± 4.0
$26_{0,26} \rightarrow 25_{0,25}$	240874.70	31	0.77	2.2 ± 0.8[g]	-23.5 ± 5.0	19.9 ± 5.0
$27_{0,27} \rightarrow 26_{0,26}$	249871.73	30	0.77	1.7 ± 0.6[g]	-26.0 ± 4.8	20.4 ± 4.8

Notes.
[a] η_b for the SMT and IRAM data and η_c for the 12 m data (see the text).
[b] Reported error ranges are 3σ; ARO 12 m data unless indicated.
[c] Partially blended line.
[d] IRAM data.
[e] Contaminated line.
[f] From Cernicharo et al. 2004; partially blended with $^{29}SiC_4$.
[g] ARO SMT data.

and an analysis of the abundance and distribution of potassium cyanide, and its implications for refractory chemistry in circumstellar gas.

2. OBSERVATIONS

Initial observations of KCN were conducted between 2001 November and 2003 June using the ARO 12 m telescope on Kitt Peak, AZ. For these measurements, dual polarization, single-sideband SIS receivers were employed in the 2 mm (130–178 GHz) and 3 mm (85–115 GHz) regions. Image rejection of typically 20 dB was achieved by tuning the mixer backshorts. Additional observations at 3 mm (84–115 GHz) were then carried out between 2008 November and 2010 January using the ARO 12 m telescope with a new, dual polarization receiver employing ALMA-type Band 3 sideband-separating SIS mixers. In this case, image rejection was >18 dB, intrinsic in the mixer architecture. System temperatures ranged from 150 K to 250 K in good weather conditions. The backends used at the 12 m were 256-channel filter banks with 1 and 2 MHz spectral resolutions, respectively, configured in parallel mode for the two receiver polarizations. The temperature scale at the 12 m is $T_R{}^*$, the chopper-wheel value corrected for forward spillover losses, where $T_R = T_R{}^*/\eta_c$, and η_c is the "corrected" beam efficiency.

Observations at 1 mm were also carried out with the ARO Submillimeter Telescope (SMT) on Mt. Graham, AZ. In this case, the dual polarization receiver consisted of ALMA-type Band 6 sideband-separating SIS mixers. Image rejection was typically >16 dB for this receiver. The backend used was a 2048-channel filter bank with 1 MHz resolution, configured in parallel mode (2 × 1024 channels). At the SMT, the temperature scale is measured as $T_A{}^*$, obtained by the chopper-wheel method. The radiation temperature is then defined as $T_R = T_A{}^*/\eta_b$, where η_b is the main beam efficiency.

All ARO data were taken in beam switching mode with a $\pm 2'$ subreflector throw. Local oscillator shifts were performed at all frequencies to check for image contamination. Pointing was routinely checked using nearby planets.

Additional observations were done with the IRAM 30 m telescope, most of them during several sessions after 2002. Dual polarization SIS receivers operating at 3 and 2 mm were used in single-sideband mode with image rejections $\geqslant$20 dB. A 512-channel filter bank was used as backend providing a spectral resolution of 1 MHz. To ensure flat baselines, observations were done in the wobbling switching mode with the secondary mirror nutating by $\pm 90''$ at a rate of 0.5 Hz. The temperature scale is measured in $T_A{}^*$, i.e., antenna temperature corrected for atmospheric absorption and for antenna ohmic and spillover losses. Pointing and focus were checked every 1–2 hr against planets or the quasar OJ 287.

The position for IRC+10216 is $\alpha = 9^h47^m57.4^s$, $\delta = 13^\circ16'44''$ [J2000.0]. Rest frequencies, beam sizes, and beam efficiencies are given in Table 1.

3. RESULTS

KCN is a T-shaped asymmetric top species with strong a-dipole-allowed transitions (Törring et al. 1980). Every transition $J \rightarrow J$–1 consists of multiple K components, labeled by K_a and K_c. The most favorable lines are those with $K_a = 0$. As summarized in Table 1, eight transitions with $K_a = 0$ were sought, ranging from the $J_{Ka,\,Kc} = 9_{0,9} \rightarrow 8_{0,8}$ line at 85 GHz to the $27_{0,27} \rightarrow 26_{0,26}$ line at 250 GHz. Six of these transitions were detected with comparable intensities (a few mK), as shown in Figure 1, which displays the ARO 12 m data. The final two transitions, $15_{0,15} \rightarrow 14_{0,14}$ and $9_{0,9} \rightarrow 8_{0,8}$, are obscured by other molecular lines (NaCN, C_5H, H_2CO, and unidentified emission) such that no distinguishable feature can be discerned. Two of the $K_a = 0$ lines were also observed with the IRAM 30 m,

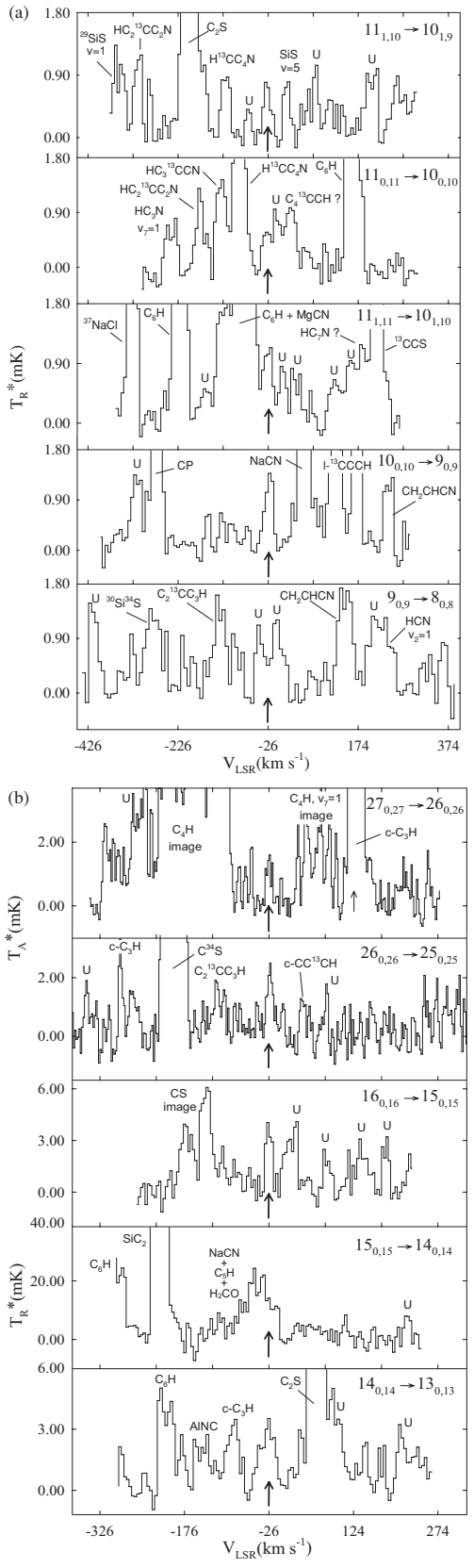

Figure 1. Spectra of the 10 rotational transitions of KCN observed toward the circumstellar shell of IRC+10216, using the ARO 12 m at 2 and 3 mm ($J_{Ka,Kc} = 9_{0,9} \rightarrow 8_{0,8}$ through $16_{0,16} \rightarrow 15_{0,15}$), as well as the ARO SMT at 1 mm ($26_{0,26} \rightarrow 25_{0,25}$ and $27_{0,27} \rightarrow 26_{0,26}$). Spectral resolution is 2 MHz for all data. Integration times are (from the lower panel to the top panel). (a) 116 hr, 217 hr, 231 hr, 288 hr, and 250 hr; and (b) 77 hr, 15 hr, 50 hr, 92 hr, and 65 hr. Emission from other molecules are labeled in the spectra, with "U" indicating unidentified features.

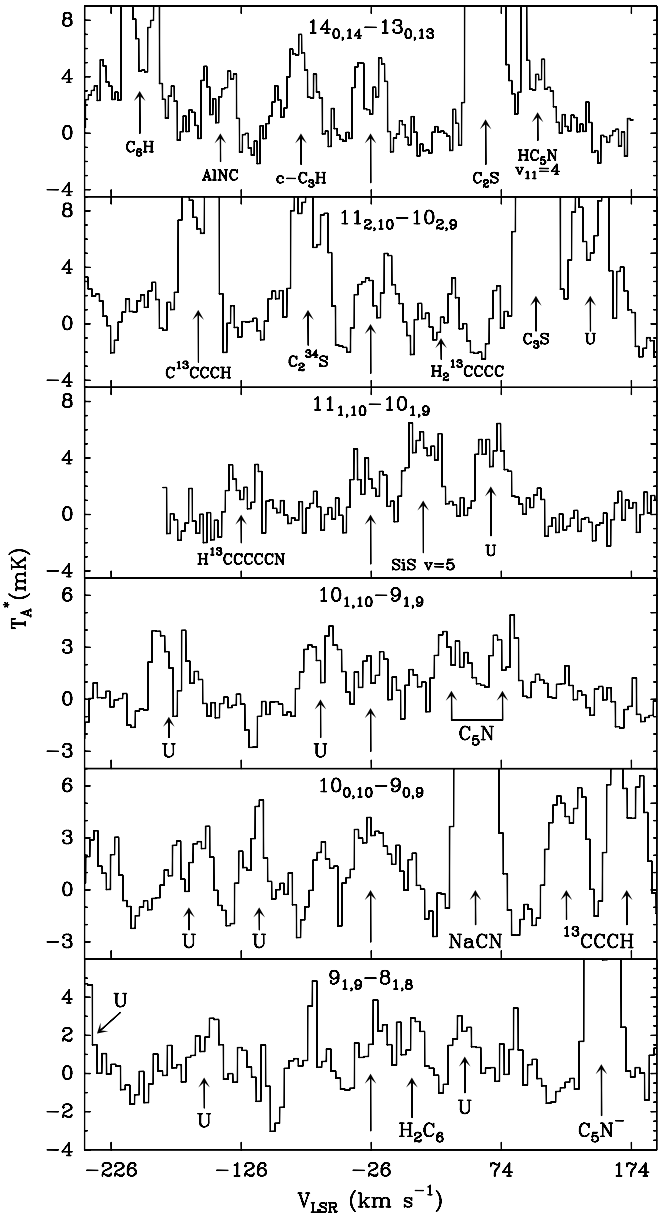

Figure 2. Spectra of the six rotational transitions of KCN observed toward the circumstellar shell of IRC+10216, using the IRAM 30 m telescope. The resolution of the data is 1 MHz. The $14_{0,14} \rightarrow 13_{0,13}$ transition is clearly U-shaped, indicating optically thin, resolved shell emission in a 19″ beam.

as shown in Figure 2. In addition, five $K_a = 1$ asymmetry components were measured for the $J = 11 \rightarrow 10$, $10 \rightarrow 9$, and $9 \rightarrow 8$ transitions, as well as a $K_a = 2$ line ($11_{2,10} \rightarrow 10_{2,9}$). The $10_{1,9} \rightarrow 9_{1,8}$ transition was previously published in Cernicharo et al. (2004). As Figures 1 and 2 illustrate, both the $K_a = 1$ asymmetry doublets are present for the $J = 11 \rightarrow 10$ and $10 \rightarrow 9$ transitions, along with the $K_a = 0$ line (also see Cernicharo et al. 2004). The identification of such K-ladder structure is striking evidence for the presence of KCN in this source.

The transition frequencies for KCN were directly measured in the laboratory only over the range 2–106 GHz (Törring et al. 1980). Predictions of the $K_a = 0$ lines in the 1 mm region should be accurate to within 1 MHz, based on NaCN. For this species, a comparable T-shaped molecule, laboratory measurements were conducted only in the region 9–40 GHz (van Vaals et al. 1984). Predictions from the constants established from this data set

were accurate to within a 1 MHz for the $K_a = 0$ lines based on observations at 1 mm, although they resulted in frequency errors as large as ±15 MHz for the $K_a > 1$ transitions (see Tenenbaum et al. 2010a, 2010b). Predictions for the $K_a \neq 0$ components usually require higher order centrifugal distortion constants, which are not well determined at lower J. Hence, extrapolation to 1 mm and shorter wavelengths for such lines may not be reliable for KCN, as is the case for NaCN.

Line parameters measured for the detected KCN lines are listed in Table 1. All features are present at LSR velocities near 26.0 km s^{-1}, as expected for IRC+10216. Linewidths (FWHM) obtained for the KCN features fall in the range 20–32 km s^{-1}, and follow a distinct trend. The spectral profiles are broader (25–31 km s^{-1}) for the lower energy, $K_a = 0$ transitions, but become more narrow ($\Delta V_{1/2} \sim 20$ km s^{-1}) for the higher energy, 1 mm lines. This decrease in linewidth, or expansion velocity, with energy above ground state is consistent with the findings of Patel et al. (2009), who found tentative features of KCN, NaCN, and NaCl with linewidths near <10 km s^{-1} in the 345 GHz region. In their 1 mm survey of IRC+10216, Tenenbaum et al. (2010a) also found very narrow lines for KCl, with $V_{\rm exp} < 10$ km s^{-1}. Note that the $J = 26$ and 27, $K_a = 0$ levels lie at 158 K and 170 K, respectively, above the ground state.

The intensities of the KCN lines are typically weak—no more than 6 mK, with many features about 1 mK. Several of the ARO spectra shown in Figure 1 were obtained with over 200 hr of integration time, and have 3σ rms noise levels of 0.3–0.5 mK. Spectral features with intensities of ∼1 mK are readily discernable in the data, with many unidentified lines. The presence of an ever-increasing number of U-lines at low noise levels in IRC+10216 is well illustrated by the recent spectral surveys of Tenenbaum et al. (2010a, 2010b) and Patel et al. (2009).

The line profiles measured with the ARO 12 m, where $\theta_b > 40''$, appear flat-topped, as do those observed with the SMT, indicative of unresolved, optically thin emission. In contrast, several of the IRAM lines appear more U-shaped, in particular the $14_{0,14} \rightarrow 13_{0,13}$ transition, measured with the smallest beam size of the data set and with the best signal-to-noise (see Figure 2). This spectrum suggests a resolved shell distribution in the 19″ beam at this frequency. The $11_{2,10} \rightarrow 10_{2,9}$ transition, measured with a 24″ beam, also looks horn shaped, while the $11_{1,10} \rightarrow 10_{1,9}$ seems more flat-topped, although it is difficult to be certain given the weak signals.

4. DISCUSSION

4.1. Abundance of KCN and Potassium Chemistry

A comparison of the intensities of the transitions measured at the ARO 12 m and the IRAM 30 m suggests a source size for KCN of ∼30″. This source distribution is consistent with the flat-topped line profiles observed for the 3 and 2 mm transitions with the 12 m telescope, where $\theta_{\rm b} \geqslant 40''$, as well as the U-shaped line observed with a 19″ beam at the 30 m. The two high energy transitions measured with the SMT, where $\theta_{\rm b} \sim 30''$, do not show a U shape, but these lines would be barely resolved in a 30″ source. Also, they lie sufficiently higher in energy with somewhat narrower line profiles, suggesting that they may arise from deeper within the stellar envelope. Given the possible observation of even higher energy transitions by Patel et al. (2009), the data seem to suggest that KCN has a shell-like distribution with $r_{\rm outer} \sim 15''$, but with an inner shell

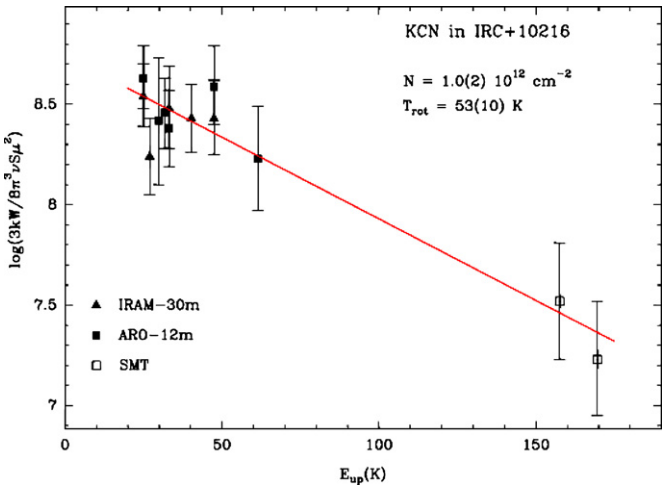

Figure 3. Rotational diagram for KCN constructed from the 14 observed transitions, assuming a source size of 30″. Data from the three telescopes involved are indicated by triangles (IRAM 30 M), filled squares (ARO 12 m), and open squares (ARO SMT).

(A color version of this figure is available in the online journal.)

radius closer to the star than found for radicals such as MgNC. This type of source distribution has also been found for another metal cyanide, AlNC (Ziurys et al. 2002).

Collisional cross sections of KCN are not known. Consequently, a rotational diagram analysis was constructed to derive an abundance, corrected for the projected source size of 30″, as shown in Figure 3. A dipole moment of 9.96 D was assumed, based on calculations by H. P. S. Mueller (see the CDMS database). This analysis produced consistent results (see Figure 3), a column density estimate of $N_{\rm tot} \approx (1.0 \pm 0.2) \times 10^{12}$ cm^{-2} and a rotational temperature of $T_{\rm rot} = 53 \pm 10$ K. Adopting a mass loss rate of 3×10^{-5} solar masses yr^{-1} and a distance of 150 pc (Agúndez & Cernicharo 2006), the H_2 column density in the shell 5–15″, where most of the KCN emission originates, is 1.8×10^{21} cm^{-2}, yielding a fractional abundance, relative to H_2, of $f \sim 6 \times 10^{-10}$.

The only other known interstellar potassium-containing molecule is KCl, also identified solely in IRC+10216. Unlike KCN, KCl is likely confined to the inner part of the circumstellar envelope, with $r \sim 5''$, mimicking the distribution of NaCl (Guélin et al. 1997). The fractional abundance of KCl in IRC+10216 is unclear. The original (rough) estimate was 3×10^{-9} (Cernicharo & Guélin 1987), but a reanalysis suggests $f \sim 4 \times 10^{-10}$ (Mauron & Huggins 2010; Highberger & Ziurys 2003). The abundance of KCN is thus comparable to that of KCl in IRC+10216.

The cosmic abundance of potassium is 1.3×10^{-7}, relative to H. If this abundance applies to an asymptotic giant branch (AGB) shell like that of IRC+10216, then only a few percent of the available potassium is in molecular form. The gas-phase atomic K abundance has recently been measured toward IRC+10216 by Mauron & Huggins (2010), who found K/H $\sim 5.5 \times 10^{-9}$, or K/H_2 $\sim 1.1 \times 10^{-8}$. If these three species K, KCl, and KCN are the main gas-phase carriers of potassium, then about 95% of this element must be condensed into dust grains, presumably as $KAlSi_3O_8$ (Lodders & Fegley 1999). There could be other gas-phase molecules containing potassium in IRC+10216, such KC_2. However, the chemical behavior of potassium appears to follow that of the other detectable metals in C-rich shells: the main molecular carriers are either halide or cyanide/isocyanide species (see Ziurys 2006).

Table 2
Observed Abundances of Metal Cyanides in IRC+10216

Species	Source Size (″)	Observed Abundance	Reference
KCN	30	6×10^{-10}	This work
NaCN	5	2.3×10^{-8}	Guélin et al. (1993), Highberger & Ziurys (2003)
AlNC	15	3×10^{-10}	Ziurys et al. (2002)
MgCN	40	7×10^{-10}	Ziurys et al. (1995)
MgNC	40	8.9×10^{-9}	Guélin et al. (1993), Highberger & Ziurys (2003)

4.2. Implications for Metal Cyanide Molecules in Circumstellar Gas

KCN is the fifth metal cyanide species identified in circumstellar gas, along with MgNC, NaCN, MgCN, and AlNC. A summary of these molecules and their abundances and source sizes in IRC+10216 is given in Table 2. Of the five metal cyanide species, NaCN is the only one thought to be an inner shell species (Guélin et al. 1993; Highberger et al. 2001); it is also the most abundant cyanide, with $f \sim 2 \times 10^{-8}$, for a source size of 5″. In contrast, the free radical MgNC and its metastable isomer, MgCN, occupy shell-like distributions in the outer envelope extending out to radii of 20″, with low rotational temperatures of ∼15 K (Guélin et al. 1993; Ziurys et al. 1995; Ziurys 2006). MgNC has an abundance of $\sim 9 \times 10^{-9}$, only a factor of 2.5 lower than that of NaCN. Based on its U-shaped profiles observed with the 30 m telescope, AlNC is thought to primarily exist in the outer shell of IRC+10216. Higher energy transitions ($J = 21 \rightarrow 20$) of this molecule have been detected, however, indicating a rotational temperature near 100 K (Ziurys et al. 2002). This elevated temperature suggests that the distribution of AlNC extends deeper into the shell, as well, as may be the case for KCN. Both AlNC and MgCN have somewhat lower abundances of (3–7) $\times 10^{-10}$ (see Table 2).

NaCN and MgNC have also been identified in the C-rich protoplanetary nebula, CRL2688 (Highberger et al. 2001). The latter molecule has additionally been found in the very evolved protoplanetary, CRL 618 (Highberger & Ziurys 2003). The abundances of NaCN and MgNC in these objects are only slightly less than that in IRC+10216.

In most cases, the cyanides appear more abundant than their halide counterparts. In IRC+10216, for example, the [KCN]/[KCl] ratio is ∼1.5, while [NaCN]/[NaCl] ∼ 5 (Highberger & Ziurys 2003; Mauron & Huggins 2010). The situation is even more extreme in CRL 2688, where the ratio is [NaCN]/[NaCl] ∼ 30 (Highberger & Ziurys 2003). Moreover, a halide counterpart to MgNC, such as MgCl or MgF, has yet to be detected in any source, although rest frequencies have been available for such species for many years (e.g., Anderson et al. 1994). Such molecules cannot be very abundant. On the other hand, aluminum clearly favors the halides, with [AlNC]/[AlCl] ∼ 0.003 and [AlNC]/[AlF] ∼ 0.002 (Ziurys et al. 2002; Highberger & Ziurys 2003).

The dominant role of cyanide species as metal carriers in circumstellar gas was not predicted by any chemical models. Metal halides, on the other hand, were clearly important in the calculations of Tsuji (1973), for example. Metal–CN bonds are common in nature, however. Vitamin B12 contains the Co–NC moiety, and the well-known dye "Prussian Blue" is formed from the FeCN functionality. Other metal cyanide compounds may be present in C-rich circumstellar gas and may provide an avenue by which to examine abundances of heavier metals such as iron and titanium.

The research is funded by the NSF Grant AST-09-06534. M.A. is supported by a Marie Curie Intra-European Individual Fellowship within the European Community 7th Framework Programme under grant agreement no. 235753.

REFERENCES

Agúndez, M., & Cernicharo, J. 2006, ApJ, 650, 374
Anderson, M. A., Allen, M. D., & Ziurys, L. M. 1994, ApJ, 425, L53
Cernicharo, J., & Guélin, M. 1987, ApJ, 183, L10
Cernicharo, J., Guélin, M., & Pardo, J. 2004, ApJ, 615, L145
Guélin, M., Lucas, R., & Cernicharo, J. 1993, A&A, 280, L19
Guélin, M., Lucas, R., & Neri, R. , et al. 1997, in IAU Symp. 170, CO: Twenty-Five Years of Millimeter-Wave Spectroscopy, ed. W. B. Latter (Dordrecht: Kluwer), 359
Highberger, J. L., Savage, C., Bieging, J. H., & Ziurys, L. M. 2001, ApJ, 562, 790
Highberger, J. L., & Ziurys, L. M. 2003, ApJ, 597, 1065
Kawaguchi, K., Kagi, E., Hirano, T., Takano, S., & Saito, S. 1993, ApJ, 406, L39
Lodders, K., & Fegley, B. 1999, in IAU Symp. 191, Asymptotic Giant Branch Stars, ed. T. Le Bertre, A. Lebre, & C. Waelkens (San Francisco, CA: ASP), 279
Mauron, N., & Huggins, P. J. 2010, A&A, 513, A31
Patel, N., et al. 2009, ApJ, 692, 1205
Savage, C. S., Ziurys, L. M., & Guélin, M. 2003, in 58th International Symp. on Molecular Spectroscopy, Columbus, Ohio, Paper RA09
Sofia, U. J., Cardelli, J. A., & Savage, B. D. 1994, ApJ, 430, 650
Tenenbaum, E. D., Dodd, J. L., Milam, S. N., Woolf, N. J., & Ziurys, L. M. 2010a, ApJS, 190, 348
Tenenbaum, E. D., Dodd, J. L., Milam, S. N., Woolf, N. J., & Ziurys, L. M. 2010b, ApJ, 720, L102
Tenenbaum, E. D., & Ziurys, L. M. 2009, ApJ, 694, L59
Tenenbaum, E. D., & Ziurys, L. M. 2010, ApJ, 712, L93
Törring, T., Bekooy, J. P., Meerts, W. L., Hoeft, J., Tiemann, E., & Dymanus, A. 1980, J. Chem. Phys., 73, 4875
Tsuji, T. 1973, A&A, 23, 411
Turner, B. E., Steimle, T. C., & Meerts, L. 1994, ApJ, 426, L97
Van Vaals, J. J., Meerts, W. L., & Dymanus, A. 1984, Chem. Phys., 86, 147
Ziurys, L. M. 2006, Proc. Natl Acad. Sci., 103, 12274
Ziurys, L. M., Apponi, A. J, Cernicharo, J., & Guelin, M. 1995, ApJ, 445, L47
Ziurys, L. M., Savage, C. S., Highberger, J. L., Apponi, A. J., Guelin, M., & Cernicharo, J. 2002, ApJ, 564, L45